Relativistic effects in time delay of atomic photoionization

I. A. Ivanov* and A. S. Kheifets†

Research School of Physical Sciences, The Australian National University, Canberra ACT 0200, Australia

(Received 14 March 2014; published 7 April 2014)

We study relativistic effects in the time delay of atomic photoionization using an example of the Xe atom subjected to a circularly polarized electromagnetic pulse. We find that while relativistic effects play only a fairly small role for both the ionization probabilities and the time delay of the corotating electron with the same sign of the angular momentum projection as the circularly polarized light, these effects produce substantial change in the time delay for a counter-rotating electron with the opposite sign of the angular momentum projection.

DOI: 10.1103/PhysRevA.89.043405 PACS number(s): 32.80.Rm, 32.80.Fb, 42.50.Hz

I. INTRODUCTION

Available experimental techniques such as attosecond streaking and angular attosecond streaking [1–3] added a new dimension to the traditional atomic and molecular spectroscopy: a possibility to follow development of the photoionization process in time. An essential ingredient in the attosecond streaking approach is the external infrared (IR) field (the probe pulse), which is used to set a clock that measures timing of the photoionization process. Any measuring device (a clock in this case) perturbs the system, a situation not uncommon in quantum mechanics. Presence of the IR field (which in experiments is in the range of 10^{11}–10^{12} W/cm^2) has to be correctly accounted for. This is not always an easy task, and the theoretical description of the attosecond streaking technique evolved from the original purely classical description [4], neglecting influence of atomic or molecular structure on the electron motion in the IR field, to various refinements of this picture [5–8], attempting to provide the level of accuracy necessary to correctly extract timing information from the experiments.

An altogether different idea of a clock, which may be used for the timing analysis of atomic photoionization, is the so-called Larmor clock. The Larmor clock exploits the idea of using the Larmor precession to measure the time it takes for a particle to traverse a barrier [9]. A static magnetic field is applied inside the barrier. The spin of the incident particles is polarized perpendicular to this field. The angle of the Larmor precession occurring during transmission is used as a measurement of the time spent traversing the barrier. Recently, this idea was generalized: instead of a magnetic field, which is difficult to confine within a barrier, it was proposed to use the spin-orbit interaction as a means to rotate the particle spin [10]. In simple physical terms, this idea can be understood by considering an electron with angular momentum l orbiting around the nucleus. In the reference frame associated with the electron, the nucleus moves creating magnetic field. The precession of electron spin in this field records time. The spin-orbit interaction is naturally occurring in many atoms and molecules and it can be conveniently used to clock various single-photon and multiphoton ionization processes. The spin-orbit wave packets represent another possibility for an alternative attoclock design. These wave packets are launched from a coherent superposition of the spin-orbit decoupled states of a singly ionized atom, which evolve in time with a well-calibrated period inversely proportional to the spin-orbit energy splitting [11]. This precise calibration of time presents a natural scale to study the evolution of the nonstationary multielectron wave function. Yet another process that can be used for this purpose is spin-exchange interaction, which is particularly strong in atoms with half-filled shells, which are fully spin polarized according to the Hund rule [12]. This interaction causes a large asymmetry between photoionization amplitudes to the spin-up and spin-down continuum states, which causes a significant spin rotation during ionization and can be used to clock the photoionization process.

For *ab initio* theoretical justification and verification of these ideas, one has to go beyond the usual framework used for timing analysis of atomic or molecular photoionization. So far, this analysis has been based on the nonrelativistic time-dependent Schrödinger equation (TDSE). However, both the spin-orbit interaction and the interaction of electron spin with a magnetic field are relativistic effects. In the present work, we describe an approach that takes into account most essential relativistic effects. We illustrate this approach by considering an example of the Xe atom subjected to a circularly polarized electromagnetic pulse.

The paper is organized as follows. In Sec. II we outline our theoretical model. In Sec. III we present our numerical results for the photoelectron momentum distribution, the ionization probability, and the time delay. The atomic units are used throughout the paper unless otherwise specified. The time delay is measured in attoseconds (1 as $= 10^{-18}$ s). The speed of light $c = 137.036$ in the atomic units.

II. THEORY

We consider an atom in the field of a circularly polarized electromagnetic pulse propagating in the z direction, with the electric field given by:

$$E_x = \frac{\mathcal{E}}{\sqrt{2}} f(t)\cos\omega t, \quad E_y = \frac{\mathcal{E}}{\sqrt{2}} f(t)\sin\omega t. \qquad (1)$$

Here we choose the carrier frequency $\omega = 1$ a.u. $= 27.2$ eV (close to the 17th harmonic of a 800 nm laser) and $f(t) = \cos^2(\pi t/T_1)$ is the pulse envelope. The field is present on the time interval $(-T_1/2, T_1/2)$, where $T_1 = 4T$, $T = 2\pi/\omega$ is an

*Igor.Ivanov@anu.edu.au
†A.Kheifets@anu.edu.au

optical cycle corresponding to the carrier frequency ω. The total duration of the pulse we use is thus four optical cycles, which gives the FWHM of 300 as. We will consider below the ionization process driven by the field (1) with the field strength $\mathcal{E}$ in Eq. (1) in the interval 0.01–0.1 a.u., corresponding to the range of intensities 3.5×10^{12}–3.5×10^{14} W/cm^2. For these field parameters ionization occurs in the multiphoton regime.

The magnetic field of the pulse $\boldsymbol{H}$ is related to the electric field (1) by the relation following from the Maxwell's equations:

$$\boldsymbol{H}(t) = \boldsymbol{n} \times \boldsymbol{E}(t), \tag{2}$$

where $\boldsymbol{n}$ is a unit vector along the direction of the propagation of the electromagnetic pulse.

We take into account relativistic effects using the so-called Breit-Pauli approximation [13]. In this approximation, the four-component Dirac equation is expanded in powers of a small parameter $1/c$ and the terms up to $1/c^2$ are retained. The wave function in this approximation is a two-component spinor. The Breit-Pauli version of the time-dependent Schrödinger equation for an atom in the field of a circularly polarized electromagnetic pulse takes the form:

$$i\frac{\partial \Psi}{\partial t} = (\hat{H}_0 + \hat{H}_{\rm int}(t) + \hat{H}_{\rm so} + \hat{H}_{\rm mag})\Psi. \tag{3}$$

Here $\hat{H}_0$ is the part of the Breit-Pauli Hamiltonian of the field-free atom, which does not include the electron spin. We describe the atom in a single active electron approximation, and we have for this operator:

$$\hat{H}_0 = \frac{\hat{\boldsymbol{p}}^2}{2} + U(r) - \frac{\hat{\boldsymbol{p}}^4}{8c^2} + \frac{\Delta U(r)}{8c^2}, \tag{4}$$

where $U(r)$ is an effective potential [14] of the Xe atom. The additional spin-dependent terms in Eq. (3) are the spin-orbit interaction:

$$\hat{H}_{\rm so} = \frac{dU}{dr}\frac{1}{2r}\frac{\hat{\boldsymbol{l}}\cdot\hat{\boldsymbol{s}}}{c^2}, \tag{5}$$

and the magnetic term, describing interaction of the electron spin with the magnetic field of the pulse:

$$\hat{H}_{\rm mag} = \frac{1}{c}\boldsymbol{H}(t)\cdot\hat{\boldsymbol{s}}. \tag{6}$$

The operator $\hat{H}_{\rm int}(t)$ in Eq. (3) describes interaction of the atom and the electric field of the pulse. We employ both the length and velocity forms for this operator:

$$\hat{H}_{\rm int}(t) = \begin{cases} \boldsymbol{E}(t)\cdot\hat{\boldsymbol{r}} \\ \boldsymbol{A}(t)\cdot\hat{\boldsymbol{p}}, \quad \boldsymbol{A}(t) = -\int_{-T_1/2}^{t}\boldsymbol{E}(\tau)\,d\tau \end{cases}. \tag{7}$$

We do not consider here nondipole terms in the interaction Hamiltonian. As dictated by the wave equation, for a pulse propagating in the z direction all the functions of time in Eqs. (1), (2) should, in fact, be considered as functions of $t - z/c$. By expanding these functions in powers of z/c, we obtain nondipole corrections to the Hamiltonian. These corrections are of the order of $\mathcal{E}/c$ or higher, and can be neglected for the small field intensities that we presently consider.

We seek a solution of Eq. (3) in the form:

$$\Psi(\boldsymbol{r},\sigma,t) = \sum_{l,m,\mu}^{L_{\rm max}} f_{lm\mu}(r,t)Y_{lm}(\theta,\phi)\chi_\mu(\sigma), \tag{8}$$

where $Y_{lm}(\theta,\phi)$ are the spherical harmonics and $\chi_\mu(\sigma)$ are the basis spin functions. In the present calculations we used $L_{\rm max} = 10$. The radial part of the TDSE is discretized on the grid with the step size $\delta r = 0.02$ a.u. in a box of the size $R_{\rm max} = 600$ a.u. Convergence of Eq. (8) with $L_{\rm max}$ and $R_{\rm max}$ has been tested thoroughly. To propagate the wave function (8) in time, we use the matrix iteration method developed in Ref. [15] and further tested in strong field ionization calculations [16–18]. This method can be easily modified to include additional spin degrees of freedom.

At the moment of time $t = T_1/2$, corresponding to the end of the pulse, we project the solution of the TDSE on the set of the ingoing scattering states $\psi^-_{\mu\boldsymbol{k}}$ [19] characterized by the electron asymptotic momentum $\boldsymbol{k}$ and the spin projection μ:

$$\psi^-_{\mu\boldsymbol{k}}(\boldsymbol{r},\sigma) = \sum_{l,j,m_j} i^l e^{-i\delta_j} R_{kj}(r)\phi_{ljm_j}(\hat{\boldsymbol{r}},\sigma)S^{jm_j}_{l\mu}(\hat{\boldsymbol{k}}). \tag{9}$$

Here $s = 1/2$, $\hat{\boldsymbol{r}} = \boldsymbol{r}/r$, $\hat{\boldsymbol{k}} = \boldsymbol{k}/k$, $\phi_{ljm_j}(\hat{\boldsymbol{r}},\sigma)$ describes angular and spin dependence of the wave function,

$$S^{jm_j}_{l\mu}(\hat{\boldsymbol{k}}) = \sum_m C^{jm_j}_{lm\,s\mu}Y^*_{lm}(\hat{\boldsymbol{k}}), \tag{10}$$

$C^{jm_j}_{lm\,s\mu}$ are the Clebsch-Gordan coefficients. This projection gives us the amplitudes

$$a_{\mu\boldsymbol{k}} = \langle\psi^{(-)}_{\mu\boldsymbol{k}}|\Psi(t)\rangle e^{iE_k t}, \quad t = T_1/2 \tag{11}$$

of detecting the ejected electron with the asymptotic momentum $\boldsymbol{k}$ and the spin projection μ after the end of the pulse. The squared moduli of these coefficients determine the photoelectron spectrum. The energy derivative of the phase of the coefficients (11) gives the photoelectron group delay, which is also known as the Wigner time delay [20–22], which can be conveniently expressed as:

$$\tau_0 = {\rm Im}\left(\frac{\hat{\boldsymbol{q}}}{q}\frac{\partial a_{\mu\boldsymbol{k}}}{\partial \boldsymbol{k}}\right). \tag{12}$$

Here the derivative is computed at the point $\boldsymbol{k} = \boldsymbol{q}$, corresponding to the asymptotic momentum of the photoelectron in the field-free zone and $\hat{\boldsymbol{q}} = \boldsymbol{q}/q$. The time delay τ has a transparent physical meaning [20,21]. It appears as a coefficient in the asymptotic expression for the trajectory of the crest of the electron wave packet in a given direction

$$\boldsymbol{r}(t) \sim \boldsymbol{q}(t - \tau_0) + \boldsymbol{r}'(t). \tag{13}$$

Here the term $\boldsymbol{r}'(t)$ gives a well-known Coulomb corrections to the trajectory, which grows logarithmically with t for large t. The time delay, therefore, can be interpreted as a moment of time when the photoelectron was launched on its escaping trajectory. This provides us with the information about development of the photoionization process in time.

Since the amplitudes (11) depend on the spin projection μ, so do the ionization probabilities and the time delays. This is, of course, very different from the nonrelativistic case in which such dependence is absent.

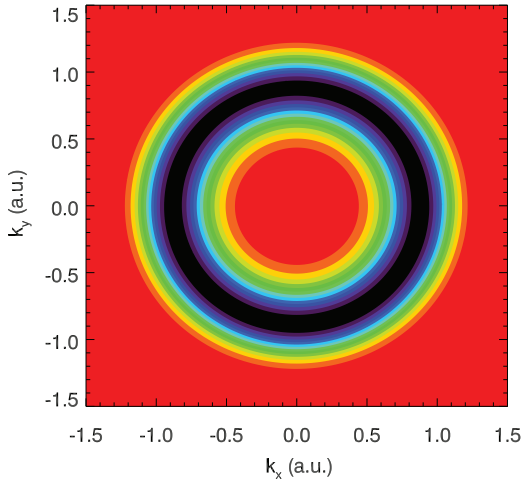

FIG. 1. (Color online) Photoelectron momentum distribution in the polarization plane for the spin up electrons. Ionization from the $5p_{3/2}$ state of Xe with $m_j = 3/2$. The peak strength of the electric field is 0.1 a.u.

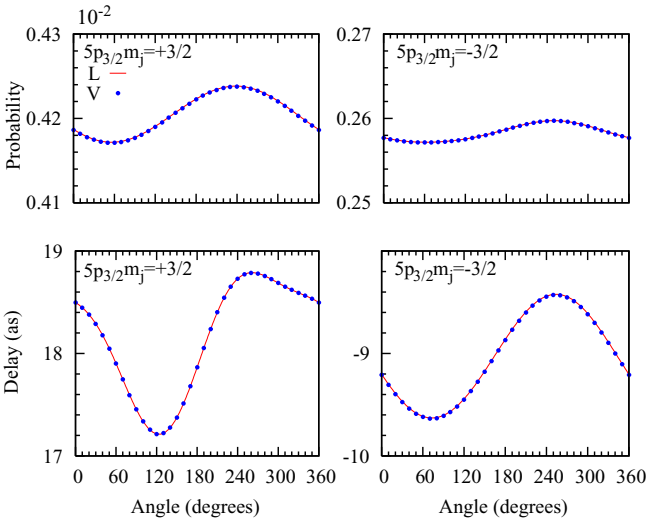

FIG. 2. (Color online) Ionization probability (top row) and time delay (bottom row) as functions of the polar angle in the polarization plane for the spin-up electrons. Solid (red) line: L-gauge calculation, filled (blue) circles: V-gauge calculation. Left and right columns show results for the $5p_{3/2}$ state of Xe with $m_j = +3/2$ and $m_j = -3/2$, respectively. The peak strength of the electric field is 0.1 a.u.

III. NUMERICAL RESULTS

We perform calculations for the Xe atom in the $5p_{j=1/2}$ and $5p_{j=3/2}$ initial states with different angular momentum projections m_j. The quantization z axis is aligned along the propagation direction of the electric field (1). The field strengths are chosen to be $\mathcal{E} = 0.01$ and 0.1 a.u., which correspond to the field intensity of 3.5×10^{12} and 3.5×10^{14} W/cm^2, respectively.

Figure 1 shows the electron momentum distribution in the polarization plane for the ionization from the $5p_{3/2}$ state of Xe with the angular momentum projection $m_j = 3/2$. We present this figure as an illustration of the general features of the photoionization process from the Xe atom. In many respects, this figure looks very much like its nonrelativistic counterpart for the ionization of the Li atom by the circularly polarized pulse that we studied in our earlier work [22]. The top panel of Fig. 2 of this work, corresponding to the field intensity $\mathcal{E} = 0.01$ a.u., shows the same uniform distribution of the ionization probability within the circle prescribed by the energy conservation. A completely uniform distribution is what the lowest-order perturbation theory (LOPT) would predict. Indeed, according to the dipole selection rules, absorption of one circularly polarized photon with $m = 1$ from the initial $5p_{3/2}$ state with $m_j = 3/2$ leads to the continuum state of even parity with $m_j = 5/2$, which can only be accommodated by $j = 5/2$. It is easy to see from Eqs. (9) and (10) that dependence of the ionization probability on the asymptotic momentum $\boldsymbol{k}$ is described in this case by a single term that contains the modulus squared of the spherical harmonic $Y_{22}(\hat{\boldsymbol{k}})$. This term produces a uniform probability distribution in the polarization plane for the only value $\mu = 1/2$ of the spin projection compatible with the even parity, $j = 5/2$ and $m_j = 5/2$. Any departure from such a uniformity can only be due to higher-order processes such as absorption of two or more photons. Such a departure from uniformity can indeed be seen at a closer inspection of Fig. 1, which we will present below.

When discussing relativistic effects, which are not very strong even in a moderately heavy Xe atom, the accuracy of the calculation becomes an important issue. We performed a series of checks of the stability of our calculation with respect to the set of numerical parameters. Convergence of our calculation was tested with respect to the parameters $L_{\max}$ and $R_{\max}$ in Eq. (8), and the step size δr used to discretize the TDSE. The numerical results obtained with $R_{\max} = 600$ a.u., $L_{\max} = 10$, and $\delta r = 0.02$ a.u. are well converged as is confirmed by a close agreement of the calculations using the length and velocity forms of the interaction Hamiltonian (7). Since both gauges weigh completely different regions of the configuration space, any lack of convergence would be immediately apparent. Such a comparison is shown in Fig. 2 where we plot the ionization probability and the time delay as functions of the polar angle in the polarization plane. The probability is obtained by integration of the photoelectron momentum distribution shown in Fig. 1 in the k_x,k_y coordinates over the radius k. Figure 2 corresponds to the ionization from the $5p_{3/2}$ state of Xe with the angular momentum projection $m_j = 3/2$. The numerical results produced by both gauges are virtually indistinguishable both for ionization probabilities and the time-delays.

To elucidate the influence of the relativistic effects, we performed two sets of calculations using the relativistic Hamiltonian Eq. (3) and its nonrelativistic limit $c \to \infty$. Such calculations are presented in Figs. 3 and 4 where we plot the ionization probability and the time delay in the polarization plane for two different values of the electric field $\mathcal{E} = 0.01$ a.u. and 0.1 a.u., respectively. Both figures present results of our calculations for the Xe $5p_{3/2}$ states with $m_j = 3/2$, spin-up electrons (left columns) and $m_j = -3/2$, spin-down electrons (right columns).

In the nonrelativistic limit, the $5p_{3/2}$ state of Xe with $m_j = 3/2$ corresponds to the $5p$ state with $m = 1$. Similarly, the state $5p_{3/2}$ with $m_j = -3/2$ corresponds to the $5p$ state with $m = -1$. The states with $m_j = 3/2$ and $m_j = -3/2$ are,

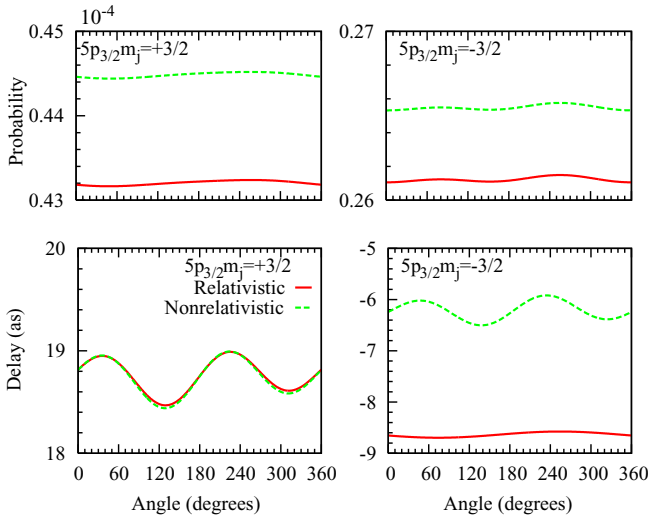

FIG. 3. (Color online) Ionization probability (top row) and time delay (bottom row) as functions of the polar angle in the polarization plane. Solid (red) line, relativistic calculation; dashed (green) line, nonrelativistic results. Left column: ionization from the $5p_{3/2}$ state of Xe with $m_j = 3/2$, spin-up electrons, right column: ionization from the $5p_{3/2}$ state of Xe with $m_j = -3/2$, spin-down electrons. The peak field strength is 0.01 a.u.

therefore, relativistic counterparts of the corotating($m = 1$) and counter-rotating ($m = -1$) nonrelativistic states, respectively. It was shown that in the nonrelativistic case the ionization probabilities for the corotating and counter-rotating electrons can be very different [23,24]. We have shown [22], that time delays for these two different initial states can differ too. The origin of this difference can be elucidated using the LOPT, which shows that it is primarily due to the difference of the corresponding Clebsch-Gordan coefficients describing angular parts of the photoionization matrix elements.

These effects are, therefore, of a nonrelativistic nature, and we can expect to see them in the relativistic calculations

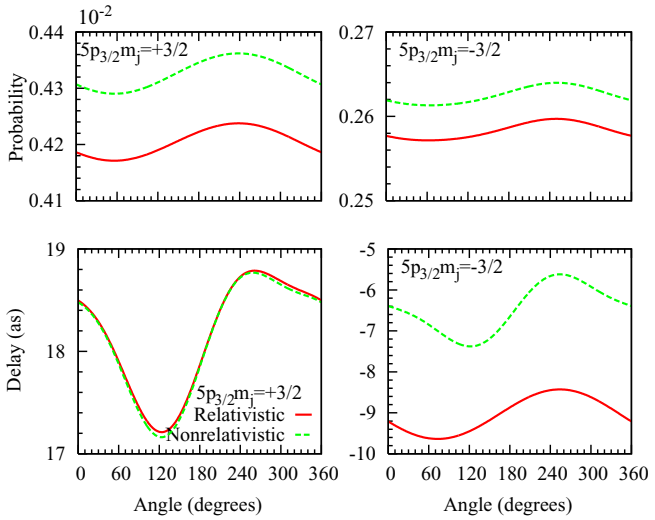

FIG. 4. (Color online) Same as Fig. 3. The peak field strength is 0.1 a.u.

for the Xe atom, which is not a deeply relativistic system. Fig. 3 and Fig. 4 show that this is indeed the case. The ionization probability for a corotating electron (left top panels) is about twice as large as for a counter-rotating one (right top panels). We also see oscillations superimposed on the flat background in the angular dependence of both the ionization probabilities and the time delays. These oscillations are present both in relativistic and nonrelativistic cases. The nature of these oscillations was elucidated in our earlier work [22] where we considered ionization of the Li atom in a similar geometry using a nonrelativistic approach. We found that for small fields, when the LOPT treatment is valid, this effect could be described as a π-periodic modulation. This modulation can be attributed to a small pulse duration giving rise to an appreciable probability of ionization processes going without energy conservation. A similar LOPT analysis can be applied to the present case. After absorption of a circularly polarized photon, the initial $5p_{3/2}$ state with $m_j = 3/2$ makes a dipole transition to the $kd_{5/2}$ continuum with $m_j = 5/2$, where the momentum k is determined by the energy conservation. This continuum state can also emit a virtual photon and thus violate the energy conservation. For a short pulse of only four optical cycles, this virtual process still has an appreciable probability. The dipole selection rules for the circularly polarized radiation lead to the $ks_{1/2}$, $kd_{3/2}$, and $kd_{1/2}$ states of even parity with $m_j = 1/2$. These states are represented in Eqs. (9) and (10) by the spherical harmonics $Y_{lm}(\hat{\boldsymbol{k}})$ with $l = 0$, $m = 0$ and $l = 2$, $m = 0,2$. These terms lead to the angular dependence of the amplitude in the polarization plane $\alpha + \beta \exp(2i\phi)$, which has a character of π modulation. This modulation is indeed seen in the time-delay plot shown on the bottom left panel of Fig. 3 for the $5p_{3/2}$ state with $m_j = 3/2$.

The angular oscillation in the time delay is different for the ionization from the $5p_{3/2}$ state with $m_j = -3/2$ for the weak field of 0.01 a.u. (the bottom right panel of Fig. 3) and for the time delays for stronger field of 0.1 a.u. (bottom row of panels of Fig. 4). Here, time-delay behavior as functions of the polar angle can rather be described as a 2π modulation. We encountered this type of modulation in the nonrelativistic case [22], for ionization by stronger fields. It can be explained as contribution of the higher-order perturbation theory effects. This explanation relies on the analysis of the contribution of the higher order terms of the perturbation theory. Such analysis can be carried with minor modifications in the present case, with the same conclusion that for stronger fields the time delays should exhibit a 2π modulation. This can explain behavior of the time delays that we observe in Fig. 4.

The case which apparently falls apart is the behavior of the time delay for ionization from the $5p_{3/2}$ state with $m_j = -3/2$ for the weak field strength of 0.01 a.u. (the bottom right panel of Fig. 3). Here the nonrelativistic calculation (dashed line) exhibits a π modulation, in agreement with the expectations based on the LOPT. The relativistic calculation, on the other hand, exhibits a 2π modulation, which we would expect to occur for higher field strengths, and which indeed occurs for this state for the field strength of 0.1 a.u. as seen in Fig. 4. For the $5p_{3/2}$ stare state with $m_j = -3/2$ relativistic effects, therefore, lead to earlier manifestation of the nonperturbative effects. We are not sure how to explain this observation.

More importantly, we see that while relativistic effects play only a fairly small role for time delays of the corotating electron (the bottom left panels of Figs. 3 and 4), they produce substantial change in the time delays for a counter-rotating electron (the bottom right set of panels). This change is of the order of 20% for the electric field strength of 0.01 a.u, and of the order of 30% for the stronger field of 0.1 a.u. This can be explained, at least qualitatively, as follows. The predominant ionization channel of the $5p_{3/2}$ state with $m_j = 3/2$ is the $kd_{5/2}$ continuum state with $m_j = 5/2$. On the other hand, the dominant ionization pathway of the $5p_{3/2}$ state with $m_j = -3/2$ is the $ks_{1/2}$ continuum state with $m_j = -1/2$. The centrifugal barrier, that keeps the continuum electron far from the nucleus, is much higher in the first case. The spin-orbit interaction decays very rapidly with the electron-nucleus distance [as r^{-3} according to Eq. (5)]. It plays, therefore, much more important role for the ionization from the $5p_{3/2}$ state with $m_j = -3/2$. That explanation is consistent with the well-known formula for the energy correction due to the spin-orbit interaction [13], which decays fast with angular momentum for large l.

To make a comparison with nonrelativistic calculation for the spin-orbit split states with arbitrary values of the total momentum j, we have to ensure a one-to-one correspondence of the relativistic and nonrelativistic initial states. This is easily achieved in the case of the states with the maximum possible j and m_j (for a given l) that we considered so far. Indeed, in the nonrelativistic limit, the $5p_{3/2}$ state with $m_j = 3/2$ corresponds to the $5p$ state with the angular momentum $m = 1$ and the spin projection $\mu = 1/2$. Similarly, the $5p_{3/2}$ state with $m_j = -3/2$ corresponds to the $5p$ state with $m = -1$, $\mu = -1/2$. The nonrelativistic limit for a state with an arbitrary j value is a linear combination of several nonrelativistic states with different projections of angular and spin momenta. The nonrelativistic limit of the relativistic $5p_{1/2}$ state with $m_j = 1/2$, for example, is a linear combination of the $5p$ states with $m = 1$, $\mu = -1/2$, and $m = 0$, $\mu = 1/2$ weighted with the corresponding Clebsch-Gordan coefficients. Taking such a superposition as an initial state in the nonrelativistic calculation, we can gauge the role of the relativistic effects. This is illustrated in Fig. 5 where we present results for the ionization from the $5p_{1/2}$ state of Xe with $m_j = 1/2$.

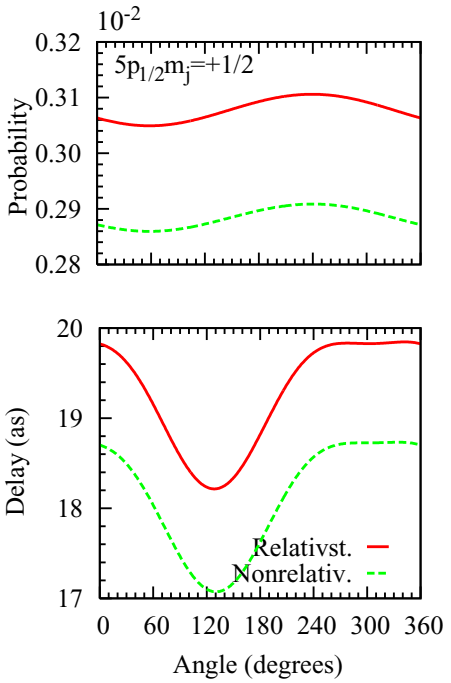

FIG. 5. (Color online) Ionization probability (top) and time delay (bottom) as functions of the polar angle in the polarization plane for the $5p_{1/2}$ state with $m_j = 1/2$ (spin up electrons). Solid (red) line, relativistic calculation; dashed (green), nonrelativistic results. The peak field strength is 0.1 a.u.

IV. CONCLUSION

We performed relativistic time-delay calculations for the photoionization of Xe atom driven by a circularly polarized electromagnetic pulse. For a moderately heavy Xe atom, relativistic effects do not play a very important role for the ionization probabilities. On the contrary, the time delays can undergo significant modifications if relativistic effects are considered. This is probably another manifestation of the general principle that the phase of the amplitude is more sensitive to small perturbations than its absolute value.

Here we considered initial electron states that are corotating and counter-rotating with respect to the electric field vector. We found that, similarly to the nonrelativistic case, the photoelectron spectra and the time delays are very different for these two orientations. As in the nonrelativistic case, the time delays exhibit modulation with respect to the polar angle in the equatorial plane. The period of this modulation is π for a weak field becoming 2π for stronger fields. The π-modulation effect can be explained as a manifestation of the processes going without energy conservation that occur for the ionization by a short pulse. The 2π modulation is due to the higher order processes. More important is the finding that while relativistic effects play only a fairly small role for ionization probabilities and time delays of the corotating electron, they produce substantial change in the time delays for a counter-rotating electron. In the latter case, the effect can reach 30%. This is a large enough effect to be taken into account in interpretation of the experiments using the Larmor clock approach. As we have seen, the magnetic field, which is a part of the measuring apparatus in the Larmor clock experiment, may itself modify the measured quantity considerably.

The present study is only the first step in elucidating the relativistic effects in time-delay calculations. Going beyond the single active electron approximation and considering relativistically many-electron effects may prove important since these effects are known to play significant role for noble-gas atoms [25]. A study relying on the relativistic random phase approximation [26] reported new effects, due to relativity, in the neighborhood of Cooper minima. Study of the truly relativistic regime of photoionization by strong laser fields as, i.e., in Ref. [27] is also of considerable interest.

ACKNOWLEDGMENT

We thank Olga Smirnova for bringing the idea of the Larmor clock to our attention. We also thank Thomas Pfeifer for discussing his work on spin-orbit wave packets with us.

The authors acknowledge support of the Australian Research Council in the form of the Discovery Grant No. DP120101805. Resources of the National Computational Infrastructure (NCI) Facility were employed.

[1] A. Baltuška, T. Udem, M. Uiberacker, M. Hentschel, E. Goulielmakis, C. Gohle, R. Holzwarth, V. S. Yakovlev, A. Scrinzi, T. W. Hänsch *et al.*, Nature (London) **421**, 611 (2003).
[2] R. Kienberger, E. Goulielmakis, M. Uiberacker, A. Baltuska, V. Yakovlev, and F. Bammer, Nature (London) **427**, 817 (2004).
[3] P. Eckle, A. N. Pfeiffer, C. Cirelli, A. Staudte, R. Dörner, H. G. Muller, M. Büttiker, and U. Keller, Science **322**, 1525 (2008).
[4] J. Itatani, F. Quéré, G. L. Yudin, M. Y. Ivanov, F. Krausz, and P. B. Corkum, Phys. Rev. Lett. **88**, 173903 (2002).
[5] S. Nagele, R. Pazourek, J. Feist, K. Doblhoff-Dier, C. Lemell, K. Tökési, and J. Burgdörfer, J. Phys. B **44**, 081001 (2011).
[6] R. Pazourek, J. Feist, S. Nagele, and J. Burgdörfer, Phys. Rev. Lett. **108**, 163001 (2012).
[7] S. Nagele, R. Pazourek, J. Feist, and J. Burgdörfer, Phys. Rev. A **85**, 033401 (2012).
[8] I. A. Ivanov and A. S. Kheifets, Phys. Rev. A **87**, 063419 (2013).
[9] B. J. Verhaar *et al.*, Physica A **91**, 119 (1978).
[10] O. Smirnova, in *International Workshop on Atomic Physics* (MPI PKS, Dresden, 2012).
[11] H. J. Wörner and P. B. Corkum, J. Phys. B **44**, 041001 (2011).
[12] V. K. Dolmatov and S. T. Manson, Phys. Rev. A **75**, 022701 (2007).
[13] I. I. Sobelman, *Introduction to the Theory of Atomic Spectra* (Pergamon Press, Oxford, 1972).
[14] A. Sarsa, F. J. Gálvez, and E. Buendia, At. Data Nucl. Data Tables **88**, 163 (2004).
[15] M. Nurhuda and F. H. M. Faisal, Phys. Rev. A **60**, 3125 (1999).
[16] A. N. Grum-Grzhimailo, B. Abeln, K. Bartschat, D. Weflen, and T. Urness, Phys. Rev. A **81**, 043408 (2010).
[17] I. A. Ivanov, Phys. Rev. A **82**, 033404 (2010).
[18] I. A. Ivanov, Phys. Rev. A **83**, 023421 (2011).
[19] V. B. Berestetskii, E. M. Lifshitz, and L. Pitaevskii, *Quantum electrodynamics* (Pergamon Press, Oxford, 1982).
[20] E. P. Wigner, Phys. Rev. **98**, 145 (1955).
[21] C. A. A. de Carvalho and H. M. Nussenzveig, Phys. Rep. **364**, 83 (2002).
[22] I. A. Ivanov and A. S. Kheifets, Phys. Rev. A **87**, 033407 (2013).
[23] K. Rzazewski and B. Piraux, Phys. Rev. A **47**, R1612 (1993).
[24] J. Zakrzewski, D. Delande, J. C. Gay, and K. Rzazewski, Phys. Rev. A **47**, R2468 (1993).
[25] A. S. Kheifets, Phys. Rev. A **87**, 063404 (2013).
[26] A. Mandal, S. Saha, P. C. Deshmukh, A. Kumar, J. Jose, and S. T. Manson, Bull. Am. Phys. Soc., http://meetings.aps.org/link/BAPS.2013.DAMOP.D1.107.
[27] M. Klaiber, E. Yakaboylu, H. Bauke, K. Z. Hatsagortsyan, and C. H. Keitel, Phys. Rev. Lett. **110**, 153004 (2013).